11th International Symposium on Turbulence and Shear Flow Phenomena (TSFP11)
Southampton, UK, July 30 to August 2, 2019

Effects of surface roughness in a turbulent plane Couette-Poiseuille flow

Jeong Hyun Kim

School of Mechanical and Nuclear Engineering,
UNIST
50 UNIST-gil, Ulsan 44919, Korea
kimjh0817@unist.ac.kr

Young Mo Lee

School of Mechanical and Nuclear Engineering,
UNIST
50 UNIST-gil, Ulsan 44919, Korea
ymlee07@unist.ac.kr

Jae Hwa Lee

School of Mechanical and Nuclear Engineering,
UNIST
50 UNIST-gil, Ulsan 44919, Korea
jhlee06@unist.ac.kr

ABSTRACT

Direct numerical simulation (DNS) of a fully developed turbulent Couette-Poiseuille flow with a rod-roughened wall is performed to investigate effects of two-dimensional (2-D) surface roughness elements. The roughness elements are periodically arranged on the bottom wall with a streamwise pitch of $\lambda = 8k$ and the roughness height is $k/h = 0.12$, where k is the roughness height. It is shown that the logarithmic law in the streamwise mean velocity profile over the rough wall Couette-Poiseuille flow is significantly shortened by the surface roughness compared to a turbulent Couette-Poiseuille flow with smooth wall. The Reynolds normal and shear stresses over the rough wall Couette-Poiseuille flow are decreased compared to that in the turbulent Couette-Poiseuille flow with smooth wall in the outer layer. These results are attributed to the weakened turbulence activity or roll-cell mode over the rough wall Couette-Poiseuille flow near the channel centerline because growth of the streamwise velocity fluctuating u-structure on the top wall is suppressed significantly, as documented through spanwise energy spectra of the streamwise velocity fluctuations.

INTRODUCTION

Turbulent Couette-Poiseuille flow can be easily seen in our life with higher diffusion efficiency and lower resistance than Poiseuille flows. These features lead to much efforts on the study of turbulent Couette-Poiseuille flows with smooth wall thus far (Pirozzoli et al., 2011). However, due to the difficulties in constructing experimental environments for such flow with surface roughness, little information has been known on Couette-Poiseuille flows with surface roughness elements. In turbulent boundary layer flows with surface roughness, Townsend (1976) argued that the turbulent motions are affected only in the vicinity of the surface roughness when the surface roughness is sufficiently small at a sufficiently large Reynolds number (Raupach et al., 1991; Jiménez et al., 2004). Schultz et al. (2007) showed that the effect of surface roughness of the three-dimensional irregular shapes is confined within 5 times of surface roughness height (k) or 3 times of effective sand grain roughness (k_s) regardless of the surface roughness height. In contrast, Burattini et al. (2008) found that the influence of surface roughness based on Reynolds stresses and skewness exists beyond the channel centerline when the one-sided 2-D rods are present in a turbulent channel flow. On the other hand, in a plane Couette flow, Aydin et al. (1991) found that there is a significant difference in Reynolds stress between the stationary wall and the moving wall when the bottom and top walls have spherical surface roughness elements.

In the present study, we investigate the effects of surface roughness on the Couette-Poiseuille flow with a one-sided rod-roughened wall. In particular, much attention is directed toward the modification of turbulence near the channel centerline for the Couette-Poiseuille flow by the surface roughness, as the longest structures residing in the channel centerline organize the entire flow field with excessively large amounts of energy for Couette-like flows (Pirozzoli et al., 2011; Avsarkisov et al., 2014; Kim and Lee, 2018). The surface roughness is placed only on the bottom wall. In order to identify the effects of the surface roughness on the Couette-Poiseuille flow, turbulent statistics (i.e., mean velocity, Reynolds stresses, time-averaged velocity fields and energy spectra of the streamwise velocity fluctuations) are analyzed, and compared with a dataset from a turbulent plane Couette-Poiseuille flow over a smooth wall (Kim and Lee, 2018).

NUMERICAL DETAILS

For an incompressible flow, the non-dimensional governing equations are

$$\frac{\partial \tilde{u}_i}{\partial t} + \frac{\partial \tilde{u}_i \tilde{u}_j}{\partial x_j} = -\frac{\partial \tilde{p}}{\partial x_i} + \frac{1}{Re}\frac{\partial^2 \tilde{u}_j}{\partial x_j \partial x_j} + f_i, \qquad (0)$$

$$\frac{\partial \tilde{u}_i}{\partial x_i} = 0 \qquad (0)$$

where $\tilde{u}_i$ represents the corresponding total velocity components and x_i denotes the Cartesian coordinates. Throughout this study, x, y, and z refer to the main flow direction, the direction perpendicular to the wall surface, and the spanwise direction, and

u, v, and w denote the corresponding velocity fluctuations in each cdirection. All variables are normalized by the laminar channel centerline velocity (U_{co}) and the channel half-height (h), and the Reynolds number is defined as $Re = U_{co}h/\nu = 7200$. The immersed boundary method is used to describe the surface roughness in the Cartesian coordinates with a rectangular domain (Kim et al., 2001). The discrete-time momentum forcing f_i is explicitly calculated in time to impose a no-slip condition on the immersed boundary. The roughness elements are periodically arranged on the bottom wall with a streamwise pitch of $\lambda = 8k$ and the roughness height (k) and width (w) are $k/h = w/h = 0.12$, leading to a fully rough state. Two streamwise locations (I and II) are defined to examine the streamwise variations of the turbulent statistics: I, the center of the roughness valley, and II, the center of the roughness crest. The bottom wall is stationary and γ indicates the moving velocity on the top wall ($\tilde{u}_M$) normalized by the centerline laminar velocity, $\gamma = \tilde{u}_M / U_{co}$. u_{tS} and u_{tM} denote the local friction velocity on the bottom and top walls for each flows, respectively. No-slip condition is used for the wall surface and periodic boundary conditions are applied in the streamwise and spanwise directions. The domain size for the calculation is (L_x, L_y, L_z) = ($40\pi h$, $2h$, $6\pi h$) and the number of grids is (N_x, N_y, N_z) = (4096, 179, 1024). The sampling time is sufficient to allow particles to travel through the streamwise dimensions at the bulk velocity more than three times.

RESULTS AND DISCUSSION

The mean streamwise velocity profiles normalized by the local bottom wall friction velocity (u_{tS}) are shown in figure 1(a). Hereafter, the statistics normalized by u_{tS} are expressed with a supercript +. C-type and CR-type indicate Couette-Poiseuille flow with a smooth wall and Couette-Poiseuille flow with a roughness element respectively. The virtual origin ($\varepsilon/k \approx 0.5$) is defined as the origin of the wall-normal distance (Jackson, 1981) and the wall-normal distance from the virtual origin is defined as $y' = y\text{-}\varepsilon$. For the C-type in figure 1(a), a long logarithmic layer with $\kappa = 0.41$ and $B = 5.0$ is observed up to the channel centerline despite the Reynolds number is low. However, for the CR-type, it is apparent that the logarithmic layer is significantly shortened compared to the that for the C-type and the profiles does not extend to the channel centerline. Due to the surface roughness, it is clear a downward shift of the mean velocity profile for the CR-type.

The streamwise Reynolds normal and Reynolds shear stress profiles normalized by u_{tS} are presented in figures 1(b) and (c). Here, the angle brackets denote average in time and in the spanwise direction. For the C-type, nearly constant Reynolds stress lines are shown in both figures 1(b) and (c) near the channel centerline. Kim and Lee (2018) reported that the increase of the Reynolds stresses in the outer region for the C-type is due to the growth of near-wall u-structures into the opposite wall on the bottom and top walls respectively. For the CR-type, both the Reynolds stress profiles are well collapsed above $y = 3k$ regardless of the streamwise locations I and II, indicating that the upper limit of the roughness sublayer is $y = 3k$ by the definition of Bhaganagar et al. (2004). The most interesting feature is that the Reynolds stresses for the CR-type are decreased compared to that for C-type in the outer layer, implying that the very-large-scale structures residing near the channel core region for the C-type are weakened by the 2-D rod roughness. Note that excessive Reynolds shear stress for the CR-type compared to that of C-type in the roughness valley is observed.

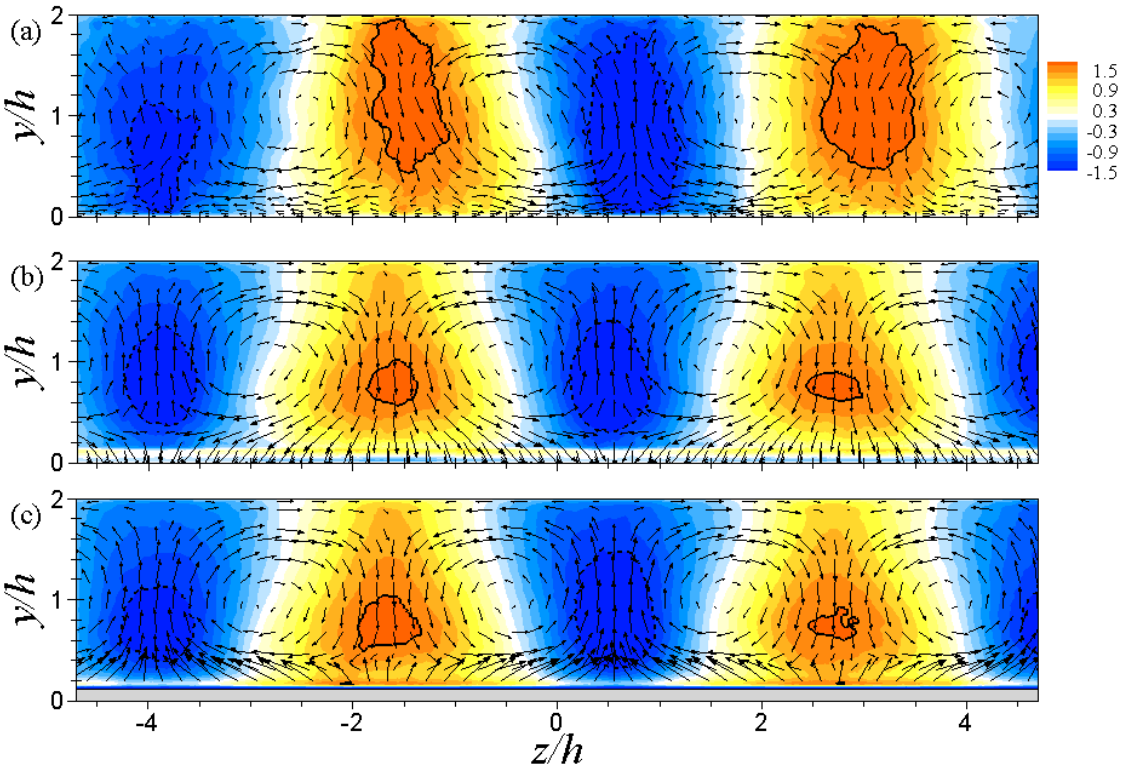

Figure 2. Temporally averaged u-structures ($\langle u \rangle_t/u_{tS}$) with velocity vectors constructed using time averaged mean wall-normal ($\langle v \rangle_t/u_{tS}$) and spanwise velocities ($\langle w \rangle_t/u_{tS}$) on the yz plane: (a) C-type, (b) CR-type (I) and (c) CR-type (II). Only part of the entire spanwise domain is depicted. In each figure, line contours of $\langle u \rangle_t/u_{tS}$ =1.5 (solid lines) and -1.5 (dashed lines) are visible to highlight the strong u-motions.

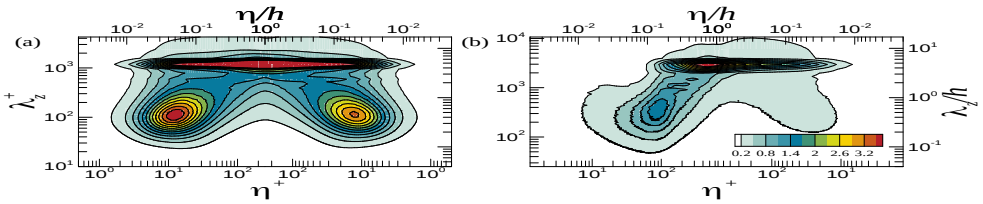

Figure 3. Pre-multiplied 2-D spanwise energy spectra of the streamwise velocity fluctuations ($k_z\Phi_{uu}/u_{tS}^2$): (a) C-type and (b) CR-type. The contour level for all types is shown in (b).

In figure 2, the temporally averaged u-structures for the C- and CR-types with time-averaged v and w vectors are drawn to investigate the turbulence activity associated with the different features of Reynolds stresses in the outer region for the C- and CR-types in figure 1. Here, the angle brackets with subscript of t denote average only in time. Red and blue areas indicate positive and negative u-structures and small portion of the entire spanwise domain is plotted for simplicity. In figure 2(a) for the C-type, large-scale patterns of high- and low-momentum are clearly observed, consistent with the previous experimental and numerical studies (Pirozzoli et al., 2011 and Avsarkisov et al., 2014). In addition, strong positive and negative u-structures are

towered on the top and the bottom walls respectively. In figures 2(b) and (c) for the CR-type, it is clear that large-scale patterns are also observed, even though the surface roughness is imposed. However, it is shown that the strength of the large-scale structures is reduced by the surface roughness (see the contour level), with detached strong positive *u*-structure on the top wall, leading to the decrease of the Reynolds stresses near the centerline. In figure 2(a) with vector fields, the existence of roll-cell modes for the strong regions of positive and negative *u*-structures is clear. Since roll-cell mode is known to be associated with large-scale structures (Hutchins and Marusic, 2007), the decreased Reynolds shear stress for the CR-type in the outer region is mainly by weakened roll-cell mode for the CR-type.

To further examine the origin of the reduced large-scale activity, the spanwise energy spectra of the streamwise velocity fluctuations are investigated. Here, the one-sided wavenumber spectrum of the streamwise velocity fluctuations Φ_{uu} is pre-multiplied by spanwise wavenumber k_z. A new vertical coordinate η is defined for a better understanding of energy spectra with respect to channel centerline;

$$\begin{aligned} \eta &= y \quad \text{where} \quad 0 \le y \le h \\ \eta &= 2h - y \quad \text{where} \quad h < y \le 2h. \end{aligned} \tag{0}$$

For the C-type, two inner peaks are visible at each bottom and top wall which is quite similar to those in a pure turbulent Poiseuille flow. The most outstanding feature in the energy spectra for the C-type is a clear outer peak located at the channel centerline with a wavelength of approximately λ_z/h = 4.6, demonstrating presence of very long motions residing near the channel centerline with excessive amount of energy. For the CR-type, however, the overall characteristics are totally different. The inner peak energy near the bottom for the CR-type decreases considerably compared to that of the C-type due to the breakup of streamwise vortices by the surface roughness (Schultz et al., 2007). Furthermore, the inner peak energy near the top wall is absent due to the surface roughness, showing that the growth of the streamwise velocity fluctuating *u*-structure on the top wall is suppressed significantly. The suppressed development of the near-wall structures on the top wall results in the weakened large-scale activity for the CR-type, leading to the decrease of the Reynolds stresses.

SUMMARY AND CONCLUSIONS

In this study, DNS of a turbulent plane Couette-Poiseuille flows with a one-sided rod-roughened wall was performed to investigate the effects of the surface roughness on the flow characteristics. Although the logarithmic layer in the mean velocity profile for the C-type is elongated through channel centerline compared to that in a pure Poiseuille flow, the wall-normal extent of the logarithmic layer for the CR-type is significantly shortened. For the Reynold stress profiles in the outer layer, the magnitude is decreased for the CR-type compared to the C-type. The temporally averaged *u*-structures revealed that the decrease of the Reynolds stresses in the outer region for the CR-type is attributed to the weakening effects of the large-scale features. In order to examine a possible cause for the weakened large-scale activity near the centerline, the spanwise energy spectra of the streamwise velocity fluctuations were analyzed. The results showed that although a secondary outer peak is observed near the centerline for the C- and CR-types, the suppression of the growth of the *u*-structure on the top wall leads to the weakened roll-cell mode, and thus the decreased Reynolds stresses.

Acknowlegements

This research was supported by the National Research Foundation of Korea (NRF) funded by the Ministry of Education (NRF-2017R1D1A1A09000537) and the Ministry of Science, ICT & Future Planning (NRF-2017R1A5A1015311).

REFERENCES

Avsarkisov, V., Hoyas, S., Oberlack, M., and Garcia-Galache, J. P., 2011, "Turbulent plane Couette flow at moderately high Reynolds number", *J. Fluid Mech.*, Vol. 751, pp. 534-563.

Aydin, E. M., and Leutheusser, H. J., 1991, "Plane-Couette flow between smooth and rough walls", *Experiments in Fluids*, Vol. 11, pp. 302-312.

Bhaganagar, K., Kim, J., and Coleman, G., 2004, "Effect of roughness on wall-Bounded turbulence", *Flow, turbulence and combustion*, Vol. 72, pp. 463-492.

Burattini, P., Leonardi, S., Orlandi, P., and Antonia, R. A., 2008, "Comparison between experiments and direct numerical simulations in a channel flow with roughness on one wall", *J. Fluid Mech*., Vol. 600, pp. 403-426.

Hutchins, N., and Marusic, I., 2007, "Large-scale influences in near-wall turbulence", *Phil. Trans. R. Soc. Lond.* A, Vol. 365, pp. 647-664.

Jackson, P. S., 1981, "On the displacement height in the logarithmic profiles", *J. Fluid Mech*., Vol. 111, pp. 15–25.

Jiménez, J., 2004, "Turbulent flows over rough walls", *Annu. Rev. Fluid Mech*., Vol. 36, pp. 173-196.

Kim, J. H., and Lee, J. H., 2018, "Direct numerical simulation of a turbulent Couette-Poiseuille flow: Turbulent statistics", *Int. J. Heat Fluid Flow*, Vol. 72, pp. 288–303.

Kim, J., Kim, D., and Choi, H., 2001, "An immersed boundary finite-volume method for simulations of flow in complex geometries", *J. Comput. Phys*., Vol. 171, pp. 132–150.

Raupach, M. R., Antonia, R. A., and Rajagopalan, S., 1991, "Rough-wall turbulent boundary layers", *Appl. Mech. Rev*., Vol. 44, pp. 1-25.

Pirozzoli, S., Bernardini, M., and Orlandi, P., 2011, "Large-scale motions and inner/outer layer interactions in turbulent Couette-Poiseuille flows", *J. Fluid Mech*., Vol. 680, pp. 534-563.

Schultz, M. P., and Flack, K. A., 2007, "The rough-wall turbulent boundary layer from the hydraulically smooth to the fully rough regime", *J. Fluid Mech*., Vol. 580, pp. 381–405.

Townsend, A. A., 1976, *The Structure of Turbulent Shear Flow*, 2nd ed. Cambridge University Press.